JOURNAL OF THE AMERICAN CHEMICAL SOCIETY

Subscriber access provided by University of South Dakota

Article

Fast Growth of Strain-free AlN on Graphene-buffered Sapphire

Yue Qi, Yunyu Wang, Zhenqian Pang, Zhipeng Dou, Tongbo Wei, Peng Gao, Shishu Zhang, Xiaozhi Xu, Zhenghua Chang, Bing Deng, Shulin Chen, Zhaolong Chen, Haina Ci, Ruoyu Wang, Fuzhen Zhao, Jianchang Yan, Xiaoyan Yi, Kaihui Liu, Hailin Peng, Zhiqiang Liu, Lianming Tong, Jin Zhang, Yujie Wei, Jinmin Li, and Zhongfan Liu

J. Am. Chem. Soc., **Just Accepted Manuscript** • DOI: 10.1021/jacs.8b03871 • Publication Date (Web): 03 Sep 2018

Downloaded from http://pubs.acs.org on September 3, 2018

Just Accepted

"Just Accepted" manuscripts have been peer-reviewed and accepted for publication. They are posted online prior to technical editing, formatting for publication and author proofing. The American Chemical Society provides "Just Accepted" as a service to the research community to expedite the dissemination of scientific material as soon as possible after acceptance. "Just Accepted" manuscripts appear in full in PDF format accompanied by an HTML abstract. "Just Accepted" manuscripts have been fully peer reviewed, but should not be considered the official version of record. They are citable by the Digital Object Identifier (DOI®). "Just Accepted" is an optional service offered to authors. Therefore, the "Just Accepted" Web site may not include all articles that will be published in the journal. After a manuscript is technically edited and formatted, it will be removed from the "Just Accepted" Web site and published as an ASAP article. Note that technical editing may introduce minor changes to the manuscript text and/or graphics which could affect content, and all legal disclaimers and ethical guidelines that apply to the journal pertain. ACS cannot be held responsible for errors or consequences arising from the use of information contained in these "Just Accepted" manuscripts.

ACS Publications

is published by the American Chemical Society. 1155 Sixteenth Street N.W., Washington, DC 20036
Published by American Chemical Society. Copyright © American Chemical Society. However, no copyright claim is made to original U.S. Government works, or works produced by employees of any Commonwealth realm Crown government in the course of their duties.

1
2
3
4
5
6
7
8
9
10
11
12
13
14
15
16
17
18
19
20
21
22
23
24
25
26
27
28
29
30
31
32
33
34
35
36
37
38
39
40
41
42
43
44
45
46
47
48
49
50
51
52
53
54
55
56
57
58
59
60

National Laboratory for Molecular Sciences, Peking University, Beijing 100871, China
Chen, Shulin; Center for Nanochemistry (CNC), College of Chemistry and Molecular Engineering, Peking University, Beijing 100871, China; Electron Microscopy Laboratory, School of Physics, Peking University, Beijing 100871, China; International Center for Quantum Materials, Peking University, Beijing 100871, China
Chen, Zhaolong; Center for Nanochemistry (CNC), College of Chemistry and Molecular Engineering, Peking University, Beijing 100871, China; Beijing National Laboratory for Molecular Sciences, Peking University, Beijing 100871, China
Ci, Haina; Center for Nanochemistry (CNC), College of Chemistry and Molecular Engineering, Peking University, Beijing 100871, China; Beijing National Laboratory for Molecular Sciences, Peking University, Beijing 100871, China; Academy for Advanced Interdisciplinary Studies, Peking University, Beijing 100871, China
Wang, Ruoyu; Center for Nanochemistry (CNC), College of Chemistry and Molecular Engineering, Peking University, Beijing 100871, China; Beijing National Laboratory for Molecular Sciences, Peking University, Beijing 100871, China
Zhao, Fuzhen; College of Science, China University of Petroleum
Yan, Jianchang; Research and Development Center for Solid State Lighting, Institute of Semiconductors, Chinese Academy of Sciences, Beijing 100083, China ; University of Chinese Academy of Sciences, Beijing 100049, China
Yi, Xiaoyan; Research and Development Center for Solid State Lighting, Institute of Semiconductors, Chinese Academy of Sciences, Beijing 100083, China ; University of Chinese Academy of Sciences, Beijing 100049, China
Liu, Kaihui; Center for Nanochemistry (CNC), College of Chemistry and Molecular Engineering, Peking University, Beijing 100871, China; Collaborative Innovation Centre of Quantum Matter, Beijing 100871, China.; State Key Laboratory for Mesoscopic Physics, School of Physics, Peking University, Beijing 100871, China
Peng, Hailin; Center for Nanochemistry (CNC), College of Chemistry and Molecular Engineering, Peking University, Beijing 100871, China; Beijing National Laboratory for Molecular Sciences, Peking University, Beijing 100871, China; Beijing Graphene Institute (BGI), Beijing 100095, China
Liu, Zhiqiang; Research and Development Center for Solid State Lighting, Institute of Semiconductors, Chinese Academy of Sciences, Beijing 100083, China; University of Chinese Academy of Sciences, Beijing 100049, China
Tong, Lianming; Center for Nanochemistry (CNC), College of Chemistry and Molecular Engineering, Peking University, Beijing 100871, China; Beijing National Laboratory for Molecular Sciences, Peking University, Beijing 100871, China
Zhang, Jin; Center for Nanochemistry (CNC), College of Chemistry and Molecular Engineering, Peking University, Beijing 100871, China; Beijing National Laboratory for Molecular Sciences, Peking University, Beijing 100871, China; Beijing Graphene Institute (BGI), Beijing 100095, China
Wei, Yujie; LNM, Institute of Mechanics, Chinese Academy of Sciences, Beijing, 100190, China; School of Engineering Sciences, University of Chinese Academy of Sciences, Beijing 100049, China
Li, Jinmin; Research and Development Center for Solid State Lighting, Institute of Semiconductors, Chinese Academy of Sciences, Beijing 100083, China ; University of Chinese Academy of Sciences, Beijing 100049, China
Liu, Zhongfan; Center for Nanochemistry (CNC), College of Chemistry and Molecular Engineering, Peking University, Beijing 100871, China; Beijing National Laboratory for Molecular Sciences, Peking University, Beijing 100871, China; Academy for Advanced Interdisciplinary Studies, Peking University, Beijing 100871, China ; Beijing Graphene Institute (BGI), Beijing 100095, China

1
2
3
4
5
6
7
8
9
10
11
12
13
14
15
16
17
18
19
20
21
22
23
24
25
26
27
28
29
30
31
32
33
34
35
36
37
38
39
40
41
42
43
44
45
46
47
48
49
50
51
52
53
54
55
56
57
58
59
60

SCHOLARONE™
Manuscripts

1
2
3
4
5
6
7
8
9
10
11
12
13
14
15
16
17
18
19
20
21
22
23
24
25
26
27
28
29
30
31
32
33
34
35
36
37
38
39
40
41
42
43
44
45
46
47
48
49
50
51
52
53
54
55
56
57
58
59
60

Fast Growth of Strain-free AlN on Graphene-buffered Sapphire

Yue Qi,[1,2,3] Yunyu Wang,[4,5] Zhenqian Pang,[6,7] Zhipeng Dou,[1,8,9] Tongbo Wei,[,4,5] Peng Gao,[*1,8,9,10] Shishu Zhang,[1,2] Xiaozhi Xu,[1,3,11] Zhenghua Chang,[6,7] Bing Deng,[1,2] Shulin Chen,[1,8,9] Zhaolong Chen,[1,2] Haina Ci,[1,2,3] Ruoyu Wang,[1,2] Fuzhen Zhao,[12] Jianchang Yan,[4,5] Xiaoyan Yi,[4,5] Kaihui Liu,[1,10,11] Hailin Peng,[1,2,13] Zhiqiang Liu,[4,5] Lianming Tong,[1,2] Jin Zhang,[1,2,13] Yujie Wei,[*, 6,7] Jinmin Li,[*, 4,5] and Zhongfan Liu[*,1,2, 3,13]*

1. Center for Nanochemistry (CNC), College of Chemistry and Molecular Engineering, Peking University, Beijing 100871, China
2. Beijing National Laboratory for Molecular Sciences, Peking University, Beijing 100871, China
3. Academy for Advanced Interdisciplinary Studies, Peking University, Beijing 100871, China
4. Research and Development Center for Solid State Lighting, Institute of Semiconductors, Chinese Academy of Sciences, Beijing 100083, China
5. University of Chinese Academy of Sciences, Beijing 100049, China
6. LNM, Institute of Mechanics, Chinese Academy of Sciences, Beijing, 100190, China
7. School of Engineering Sciences, University of Chinese Academy of Sciences, Beijing 100049, China
8. Electron Microscopy Laboratory, School of Physics, Peking University, Beijing 100871, China
9. International Center for Quantum Materials, Peking University, Beijing 100871, China
10. Collaborative Innovation Centre of Quantum Matter, Beijing 100871, China.
11. State Key Laboratory for Mesoscopic Physics, School of Physics, Peking University, Beijing 100871, China
12. College of Science, China University of Petroleum, Qingdao, 266580, China
13. Beijing Graphene Institute (BGI), Beijing 100095, China

Corresponding authors: Zhongfan Liu (zfliu@pku.edu.cn), Tongbo Wei (tbwei@semi.ac.cn), Peng Gao (p-gao@pku.edu.cn), Jinmin Li (jmli@semi.ac.cn), Yujie Wei (yujie_wei@lnm.imech.ac.cn)

KEYWORDS: AlN/sapphire, AlN/graphene/sapphire, graphene buffer layer, nucleation density reduction, strain relaxation

ABSTRACT: We study the roles of graphene acting as a buffer layer for growth of AlN film on sapphire substrate. Graphene can reduce the density of AlN nuclei but increase the growth rate for individual nucleus at the initial growth stage. This can lead to the reduction of threading dislocations evolved at the coalescence boundaries. The graphene interlayer also weakens the interaction between AlN and sapphire and accommodates their large mismatch in lattice and thermal expansion coefficient, thus the compressive strain in AlN and tensile strain in sapphire is largely relaxed. The effective relaxation of strain further leads to low density of defects in AlN films. These findings reveal the roles of graphene in III-nitride growth and offer valuable insights into the efficient applications of graphene in the LED industry.

1
2
3
4
5
6
7
8
9
10
11
12
13
14
15
16
17
18
19
20
21
22
23
24
25
26
27
28
29
30
31
32
33
34
35
36
37
38
39
40
41
42
43
44
45
46
47
48
49
50
51
52
53
54
55
56
57
58
59
60

Introduction

Epitaxial growth of group III-nitride films enables many optoelectronic devices such as light emitting diodes (LEDs),[1-2] laser diodes (LDs),[3] ultraviolet emitters[4] and high frequency power electronics.[5-6] With the lack of native substrates (*i.e.* GaN and AlN) at economical costs, III-nitride films are always grown heteroepitaxially on various foreign substrates, e.g., sapphire, silicon and silicon carbide,[7-9] by using the metalorganic chemical vapor deposition (MOCVD) method. Such a growth route always produces severely-stressed films with high-density defects (e.g. dislocations or stacking faults) due to the large mismatch in lattice and thermal expansion coefficient between the substrate and epilayers.[10-12] These defects could detrimentally degrade the device performance (e.g. efficiency, reliability and life) by acting as non-radiative recombination sites or leakage current pathway.[13-14] In order to achieve high-quality III-nitride films,[15-17] buffer layers of low-temperature grown AlN or GaN are generally required to minimize the mismatch effect.

Notably, in addition to the defects introduced by the lattice and thermal mismatch between the substrate and epilayers, a high density of threading dislocations (TDs) also evolve during the coalescence of separated three dimensional (3D) islands of III-nitrides. This type of TDs is always vertical to the substrate and can propagate through the thickness into the quantum well layers. It is even worse that these TDs have no possibility to react with each other to be eliminated during the subsequent thickness increase.[18] However, reducing the density of islands and simultaneously increasing the domain size at the nucleation stage are effective to reduce the density of TDs.[19-20]

In order to improve the quality of III-nitride films, many materials have been proposed to act as the buffer layers including graphene. As one of the typical two dimensional (2D) materials, graphene has no dangling bond on the surface, but possesses a hexagonal arrangement of atoms similar to (0001) c-plane of III-nitrides (e.g. AlN). Maturely, large-scale single-crystal graphene could be synthesized with the chemical vapor deposition (CVD) method.[21-23] Using graphene as the buffer layer, the effects of mismatch between AlN (or GaN) and graphene (~26.4% or ~29.6%)[24-26] are no longer significant due to the quasi-van der Waals epitaxy growth for III-nitrides on graphene. Additionally, the inert surface of graphene could weaken the nucleation of III-nitrides, and the low migration barrier of metals on graphene allows the adatoms to diffuse easily, which promotes the 2D lateral growth of nitrides islands, and thus reduces the density of TDs formed at the coalesced boundaries.[26-28] Consequently, the quality of III-nitrides synthesized through the graphene-buffered route could be comparable to that of the conventional AlN (GaN)-buffered route.[29] Moreover, benefiting from the weak interactions between graphene interlayers and graphene-epilayers, the upper LEDs could be easily transferable onto foreign substrates such as metal or plastic, to improve the thermal conductivity of device or achieve the ideal flexibility.[29-30] Nevertheless, in the graphene-buffered growth route, the roles of graphene are still ambiguous, including the effects of graphene on the growth rate and stain relaxation of nitride films. These issues are imperative for the effective applications of graphene in the LED industry.

In this work, graphene is used as the buffer layer for AlN growth on sapphire (α-Al_2O_3(0001)), and it brings two important advantages. First, with the presence of graphene, the nucleation density of AlN is decreased, and the growth rate of individual nucleus is increased. As a result, the density of TDs evolved at the coalescence boundaries is significantly reduced. Second, the strains in both AlN and sapphire are largely reduced by the introduction of graphene, which could further lower the density of misfit dislocations in the epilayers, and the enhancement of efficiency of LEDs is expected. These finding sheds lights on the growth of high-quality semiconducting nitride films via graphene engineering.

1 2 3 4 5 6 7 8 9 10 11 12 13 14 15 16 17 18 19 20 21 22 23 24 25 26 27 28 29 30 31 32 33 34 35 36 37 38 39 40 41 42 43 44 45 46 47 48 49 50 51 52 53 54 55 56 57 58 59 60

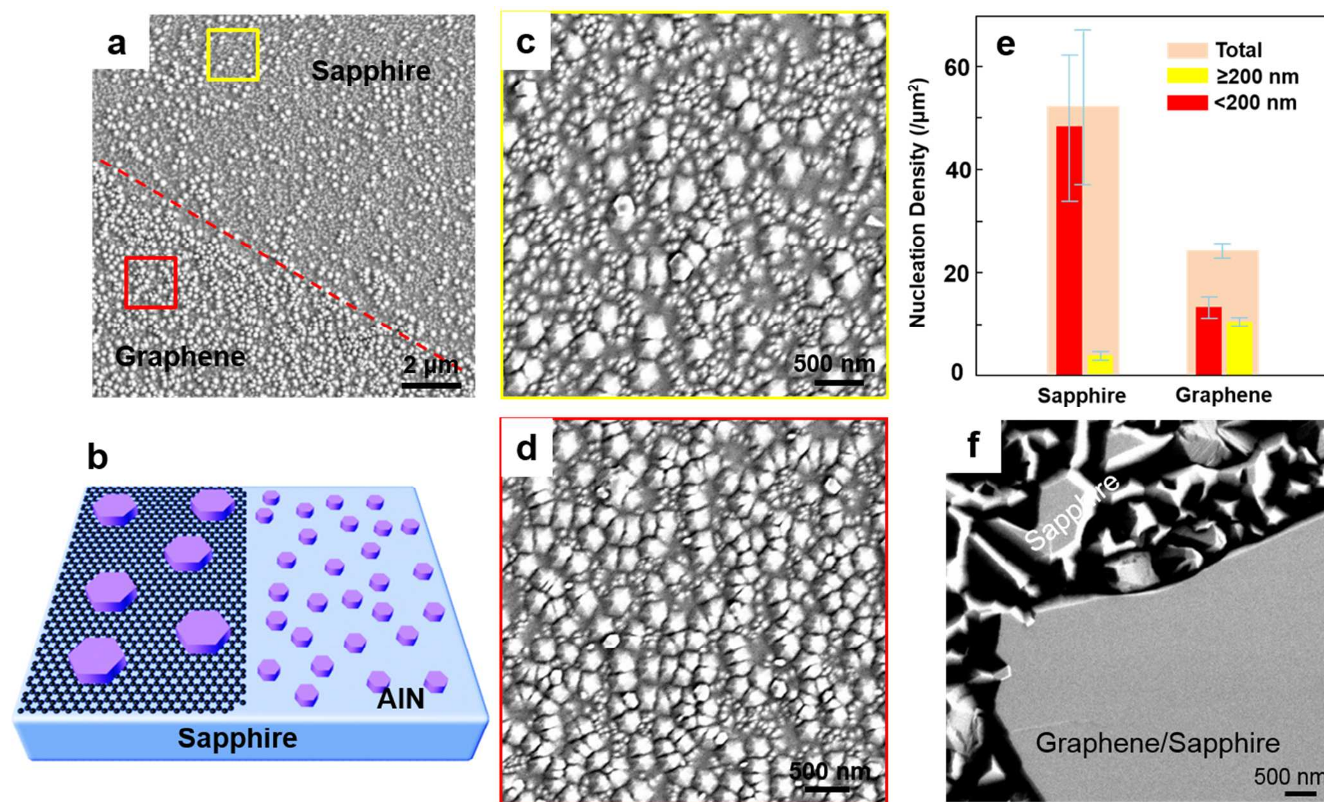

Figure 1: Effects of graphene interlayer on AlN nucleation. (a) Large-scale SEM image showing the nucleation of AlN on bare sapphire and graphene-buffered sapphire (growth duration: ~6 min). (b) The corresponding schematic. (c, d) Magnified SEM images showing the distributions of AlN nucleus on bare sapphire (c) and graphene-buffered sapphire (d). (e) Statistics of the density and size of AlN nucleus on sapphire and graphene/sapphire. (f) SEM image for non-coalesced and coalesced AlN domains on sapphire and graphene/sapphire, respectively.

Results and Discussion

Single-crystal monolayer graphene grown on Cu(111) foils was transferred onto sapphire substrate, with the surface being kept flat and clean (SEM images in **Figure S1**). The Raman spectrum of graphene transferred onto sapphire in **Figure S1e** showed low or even negligible D peak and intense narrow 2D peak, which implied the high quality of graphene.[31] Subsequently, MOCVD method was used for AlN growth on the obtained graphene/sapphire substrate. At the initial stage of growth, the graphene covering on the surface impose obvious effects on the nucleation density of AlN and growth rate of individual nucleus. The SEM image in **Figure 1a** presents AlN nucleation on bare (upper right) and graphene-covered sapphire (bottom left). The two typical regions can be easily distinguished from the different nucleation density and domain size of AlN, as schematically shown in **Figure 1b**. The statistics from the magnified SEM images in **Figure 1c** and **d** show that the nucleus densities of AlN are $41/\mu m^2$ on sapphire and $23/\mu m^2$ on graphene/sapphire (**Figure 1e**). This result implies that graphene can suppress the AlN nucleation, which is likely attributed to the lack of dangling bonds on the surface. Furthermore, the densities of AlN domain with diagonal distance larger than 200 nm on sapphire and graphene/sapphire are $3/\mu m^2$ and $11/\mu m^2$, respectively. These different growth rates of AlN on the two types of regions are possibly due to the fact that graphene could reduce diffusion barrier of metals and make adatoms diffuse easily with large diffusion lengths, which accelerates the 2D lateral growth of the islands on graphene-covered sapphire with respect to that on bare sapphire. Moreover, the same

tendency was also observed when the nucleation time was reduced to ~3 min (**Figure S2**). Notably, the orientations of the separated AlN islands on graphene/sapphire are well aligned, as evidenced by the selected area electron diffraction pattern (SAED) in **Figure S3**. In addition, AlN nucleation density could increase at the domain edges and wrinkles of graphene due to the rich dangling bonds at the domain edges and the enhanced chemical reactivity at the wrinkles, which is caused by the increased strain energy induced by the local mechanical deformation of graphene.

During the subsequent coalescence of these separated 3D islands, TDs vertical to the substrate always evolved at the coalescence boundaries. These types of TDs have no possibility to react with each other thus cannot be eliminated by increasing the thickness.[18, 32-34] In this regard, on graphene/sapphire, the lower nucleation density and larger domain size of AlN nucleus can effectively reduce the formation of TDs. When the growth duration is extended to ~60 min, AlN coalesces to form flat films on graphene/sapphire, which is in sharp contrast to the non-coalesced, rough islands on bare sapphire counterpart (SEM images in **Figure 1f** and **Figure S1f**). Notably, the Raman spectra in **Figure S4a**, **b** and **Figure S5a**, **b** prove the existence of graphene in the coalesced regions while the absence in the non-coalesced AlN regions, respectively. The cathodoluminescence (CL) spectrum from AlN/graphene/sapphire shows a narrower full width at half maximum (FWHM) and stronger intensity than that from AlN/sapphire (peaks at ~210.6 nm for AlN), indicating the higher quality of the films (**Figure S6**). The characterization of XRD rocking curve shows that with the introduction of graphene, the density of screw dislocation decreased from 8.01×10^{8} to 2.81×10^{8} cm^{-2}, and the density of edge dislocation decreased from 5.88×10^{9} to 4.63×10^{9} cm^{-2}. Notably, the new growth process of AlN films with the introduction of graphene interlayer bypasses the native buffer layers growth commonly used in the traditional two-step MOCVD method.

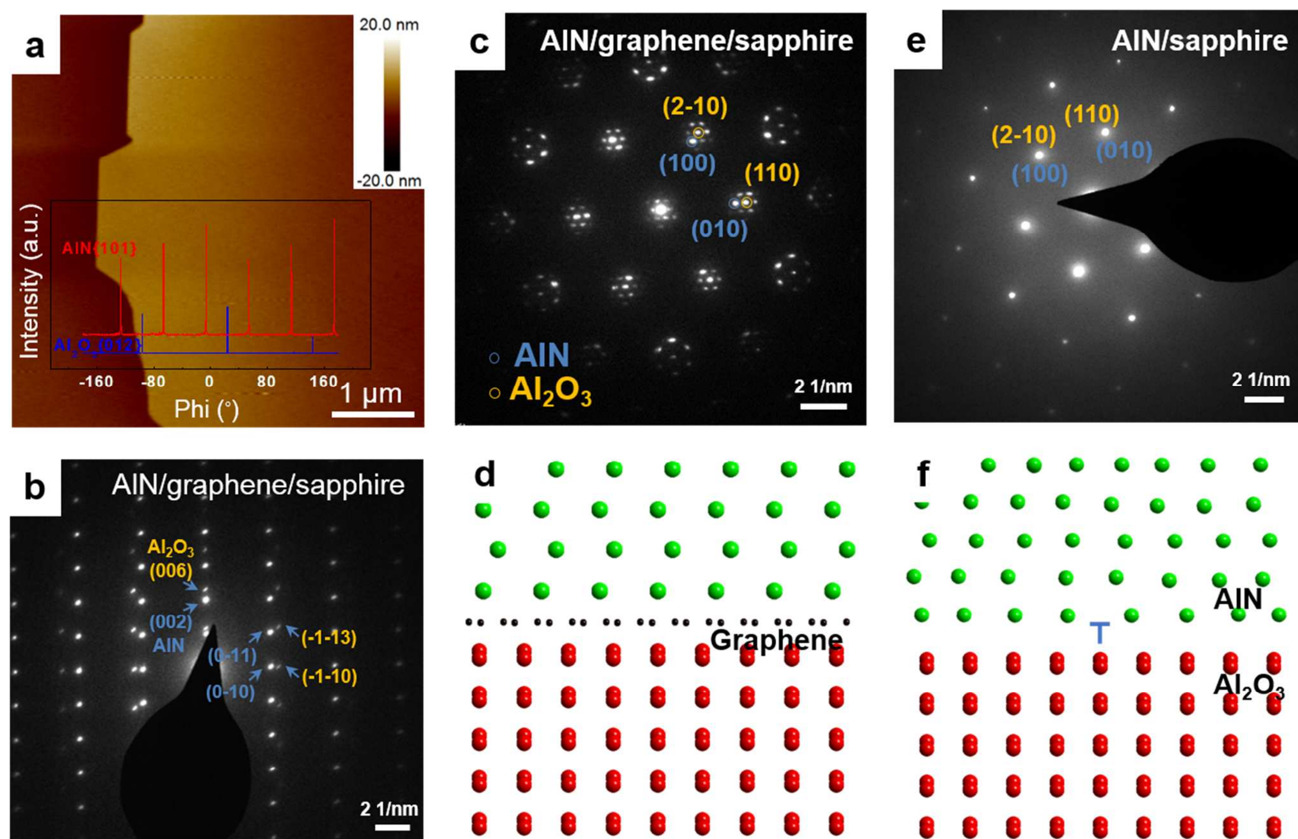

Figure 2: Effects of graphene buffer layer on the strains in AlN and sapphire. (a) AFM image for AlN films grown on graphene/sapphire. Inset: XRD phi scan of AlN/graphene/sapphire, showing

the good large-scale epitaxial relationship between AlN and sapphire. (b) SAED pattern from the interface region of AlN/graphene/sapphire cross-sectional sample. (c, e) SAED patterns of AlN/graphene/sapphire (c) and AlN/sapphire (e) planar view samples. (d, f) Schematics for the two types of interfaces. Only Al and C atoms are visible for clarity. In (b), the zone axes of sapphire and AlN are [1-10] and [100], respectively. In (c, e), the axis is along [001].

For AlN directly grown on sapphire, due to the large mismatch in lattice and thermal expansion coefficient, severe strains always remain in the film and substrate (lattice constants: a_{AlN}=0.3112 nm, $a_{sapphire}$=0.4758 nm; mean expansion coefficients along "a" axe: α_{AlN} =5.3×10^{-6}/^{o}C, $\alpha_{sapphire}$ =7.3×10^{-6}/^{o}C).[35] The graphene buffer layer can help release the strains in the film and substrate. The surface of the as-grown AlN film on graphene/sapphire is flat, presenting atomic terrace in the AFM image in **Figure 2a**. The X-ray diffraction (XRD) in **Figure S7a** and cross-sectional SAED in **Figure 2b** confirm the epitaxial relationship between AlN and sapphire and indicate that the growth direction (out-of-plane orientation) is (0002). In addition, the large-scale epitaxial growth of AlN on graphene-covered sapphire is investigated by XRD phi scan (inset in **Figure 2a**) and LEED characterizations (**Figure S7b**). In **Figure 2b**, there are two separate sets of diffraction points along the growth direction [001] and in the a/b planes, indicating that sapphire and AlN maintain their respective lattice structures, and the strain between them has been largely relaxed due to the presence of graphene. The SAED patterns along [001] direction of AlN/graphene/sapphire and AlN/sapphire plane samples are presented in **Figures 2c** and **e**, respectively. The relaxed structure in AlN/graphene/sapphire is further confirmed by the satellite spot diffraction patterns of the planar view specimen in **Figure 2c.** The satellite spots are caused by double diffraction, *i.e.*, the beams are firstly diffracted by AlN and subsequently diffracted by sapphire (or vice versa). The satellite spot diffraction patterns confirm that sapphire and AlN maintain their respective lattice structures, which also indicates the strains in AlN and sapphire are relaxed, as schematically shown in **Figure 2d**. In comparison, single set of diffraction pattern is observed for AlN on bare sapphire in **Figure 2e** for the reason that the lattice of AlN is fully clamped and aligned with the sapphire substrate. When AlN is epitaxially grown on bare sapphire substrate, the in-plane lattice of AlN is fully constrained by the sapphire substrate. Their reflections in the SAED patterns are therefore overlapped with each other, showing a single set-like patterns in **Figure 2e**. In this case, significant strain should exist in AlN, as shown in **Figure 2f**. The element mappings in **Figure S8** implied the existence of sapphrie under AlN in the sample in **Fiugre 2e**. In addition, these SAED patterns in **Figure 2c** and **e** also indicated that the graphene buffer layer did not change the orientation of AlN on sapphire. The cross sectional SAEDs of single AlN and graphene/sapphire materials are presented in **Figure S9** for reference.

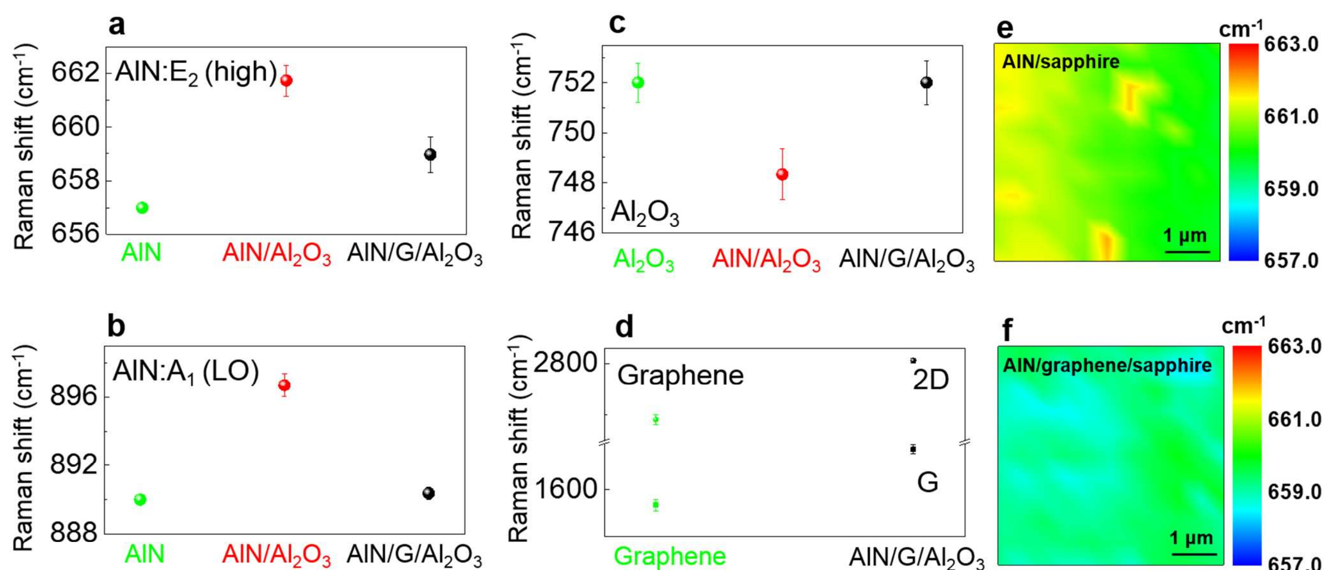

Figure 3: Strains in AlN/sapphire and AlN/graphene/sapphire characterized by Raman spectroscopy. (a, b) Relative Raman shifts of E_2 (high) (a) and A_1 (LO) (b) of AlN in pristine AlN, AlN/sapphire and AlN/graphene/sapphire, respectively. (c) Relative Raman shifts of sapphire in pristine sapphire, AlN/sapphire and AlN/graphene/sapphire. (d) Relative Raman shifts of G and 2D peaks of graphene in pristine graphene and AlN/graphene/sapphire. (e, f) Raman mappings (5 μm × 5 μm) of E_2(high) peak of AlN in AlN/sapphire and AlN/graphene/sapphire, respectively.

The strains in AlN and sapphire could impose profound effects on their Raman spectra, for example, the E_2(high) mode of AlN around 655 cm^{-1} could provide a clear signature for the biaxial strain within the basal plane.[36-38] The full spectra from the samples of bare sapphire, AlN/sapphire and AlN/graphene/sapphire are shown in **Figure S10**. For reference sapphire, there are three typical peaks at ~419.2 cm^{-1}, ~580.1 cm^{-1} and ~751.2 cm^{-1} (**Figure S10a**), and for reference AlN, the representative peaks are located around 248.0 cm^{-1} (E_2(low)), 657.0 cm^{-1} (E_2(high)) and 890.0 cm^{-1} (A_1 (LO)) (**Figure S10b** and **c**).[39-40] Specifically, from **Figure 3a** and **Figure S10d**, the strain-sensitive E_2(high) peaks from AlN/graphene/sapphire located at lower wavenumber of ~658.9 cm^{-1}, much closer to the pristine one (~657.0 cm^{-1}), compared to that of AlN/sapphire (~661.7 cm^{-1}), which suggests the compressive strain in AlN is significantly relaxed. The same conclusion can be obtained from the analysis of A_1 (LO) peaks (~890.4 cm^{-1} for AlN/graphene/sapphire, ~890.0 cm^{-1} for bulk AlN and ~896.7 cm^{-1} for AlN/sapphire (**Figure 3b** and **Figure S10e**). For sapphire in **Figure 3c**, the strain sensitive peak from AlN/graphene/sapphire is ~752.0 cm^{-1} (black), much closer to the reference one (green), while it shifts to much lower wavenumber of ~748.3 cm^{-1} (red) for AlN/sapphire, further confirming that the tensile strain in sapphire of AlN/graphene/sapphire is also reduced. **Figure 3e** and **f** are the Raman mappings (5 μm × 5 μm) of E_2(high) peak of AlN in AlN/sapphire and AlN/graphene/sapphire, respectively, which showed that at a large scale, the E_2(high) peak of AlN in AlN/sapphire shifted to much higher wavenumber, and the peak in AlN/graphene/sapphire was much closer to the pristine one. In addition, the analysis about the changes of the lattice parameters of AlN based on the XRD measurements are also presented in **Table 1** in the supporting information to illustrate the strain differences in the systems of AlN/graphene/sapphire, AlN/graphene and bulk AlN.

Notably, the 2D and G peaks of graphene also exhibit high stain sensitivity. Previous study

reported that under the uniaxial tensile strain, the 2D and G peaks of monolayer graphene present significant red shifts with 27.8 and 14.2 cm^{-1} per 1%, respectively.[41] Under the biaxial strain introduced by graphene bubbles, G peak could decrease from 1598 to 1525 cm^{-1} and 2D peak could move from 2695 to 2552 cm^{-1}.[42] In the current work, when graphene is sandwiched between AlN and sapphire, its G and 2D peaks shifted to much higher wavenumbers of ~1648.3 cm^{-1} and ~2810.3 cm^{-1}, respectively, with regard to that of the pristine ones (~1581.6 cm^{-1} and ~2676.9 cm^{-1}, respectively) (**Figure 3d**). Due to the negative expansion coefficient of graphene (~-7×10^{-6}/K) and the positive expansion coefficients of AlN and sapphire ($\alpha_{AlN} = 5.3\times10^{-6}/^{o}C$, $\alpha_{sapphire} = 7.3\times10^{-6}/^{o}C$),[35] strong compressive strain imposes graphene during cooling after MOCVD growth, which mainly account for such a large shift. The values of the peak positions in **Figure 3** are detailed in **Figure S11**.

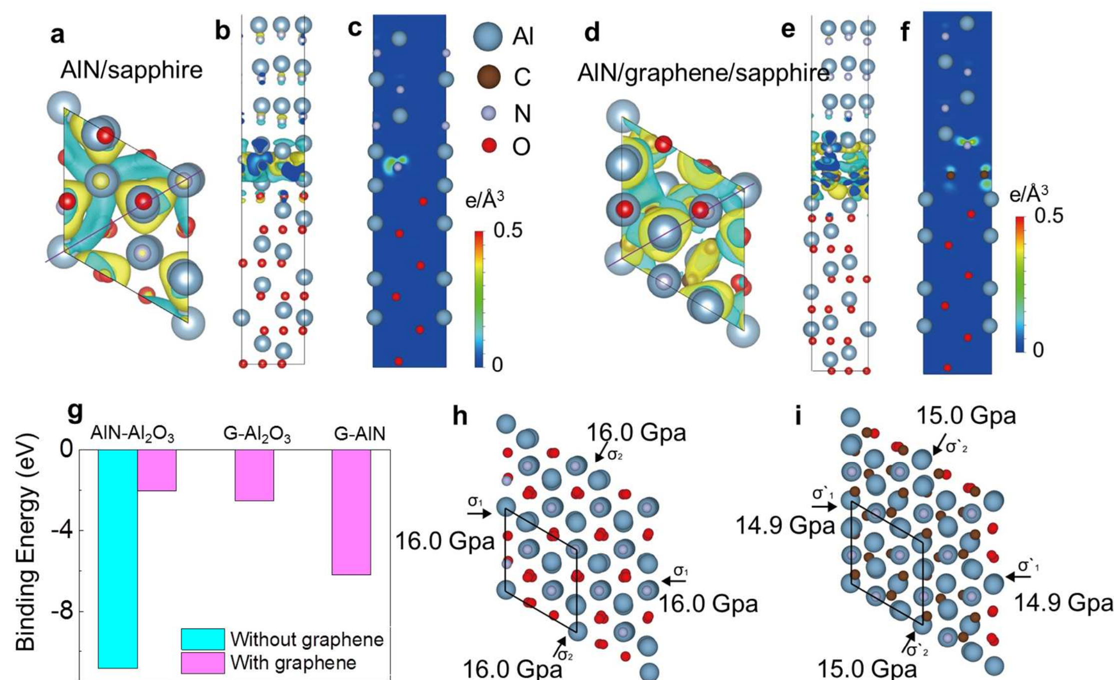

Figure 4: DFT calculations of AlN-Al_2O_3 binding energy (BE) and the internal stress in AlN. (a, d) Calculated models of AlN/sapphire and AlN/graphene/sapphire, respectively. The black parallelogram denotes the calculation cell. (b, e) Front view of 3D charge density corresponding to (a, d), respectively. The yellow and blue regions represent the electron gain and lose, respectively. (c, f) Sections of charge density along the purple line in (a, b), respectively. (Units of the contours: e/Å^3). (g) Calculated BEs for AlN-Al_2O_3 in AlN/sapphire and AlN/graphene/sapphire are -10.84 eV and -2.04 eV, respectively, and -6.20 eV for G-AlN, -2.51 eV for G-Al_2O_3. (h, i) Calculated internal stress in AlN without (g) and with (h) graphene interlayer (16.0 Gpa and 14.9 Gpa, respectively).

To better understand the roles of graphene in the strain relaxation during AlN growth on sapphire, DFT calculations are performed to extract the AlN-sapphire (AlN-Al_2O_3) binding energy (BE) and the internal stress in AlN film. **Figure 4a** and **d** are the calculated models of AlN/sapphire and AlN/graphene/sapphire, respectively. In the front view of 3D charge density in **Figure 4b** and **e**, obvious charge redistribution can be observed after graphene insertion. In AlN/sapphire, there exist prominent charge exchange between N in AlN and Al in Al_2O_3 (**Figure 4b** and **c**). After graphene insertion, the charge exchange happens among all the interfaces of graphene (G)-AlN and G-Al_2O_3 (**Figure 4e** and **f**),

and the resulted strong interactions (-2.51 eV for G-Al_2O_3 and -6.20 eV for G-AlN, **Figure 4g**) lead to the distortion of graphene layer (**Figure S12**), which can explain the strong compressive strain introduced in graphene. The calculated AlN-Al_2O_3 BEs are -10.84 eV for AlN/sapphire and -2.04 eV for AlN/graphene/sapphire (**Figure 4g**). The weakened AlN-Al_2O_3 interaction in AlN/graphene/sapphire largely accommodates their lattice and thermal mismatch, thus the compressive strain in AlN is largely released. The calculated internal stress in AlN is reduced from 16.0 Gpa in AlN/sapphire to 14.9 Gpa in AlN/graphene/sapphire (**Figure 4h** and **i**), which is in excellent agreement with electron microscopy and Raman characterizations.

Summary

In summary, the introduction of graphene buffer layer between AlN and sapphire can reduce the nucleation density and increase the growth rate of AlN nuclei. As a result, the TDs evolved at the coalescence boundaries is obviously decreased thus the film quality is increased. Simultaneously, the graphene buffer layer significantly weakens the AlN-Al_2O_3 interaction, which accommodates their large lattice and thermal mismatch. Thus the compressive strain in AlN and tensile strain in sapphire are largely relaxed. High energy efficiency of the LEDs that are fabricated from the strain-free AlN film can be expected. This work reveals the role of graphene buffer layer in III-nitrides growth, which provides instructions for the use of graphene in LED industry.

Experimental details

Graphene synthesis. Graphene was grown on Cu(111) foils through CVD method at ~1000 ^{o}C with 10 sccm CH_4 (0.1% diluted in Ar) being introduced into the system.

AlN growth. AlN film was grown with a low pressure MOCVD (~50 torr), using Trimethylaluminum (TMAl) (50 sccm) and NH_3 (500 sccm) as Al and N precursors and H_2 (12 SLM) as the carrier gas. It is a one-step process here without using LT-buffer layers, and the HT-AlN was grown at a nominal temperature of 1200 ^{o}C for 1 h.

Graphene transferring process. Poly(methyl methacrylate) (PMMA, 4 wt%) was firstly spin-coated on graphene/Cu substrates at the speed of 2000 rpm for 1 min, and cured at 170 ºC for 3 min. Then, Cu was etched using 1 mol/L $Na_2S_2O_8$ (aq) as etchant for about 1 h. After etching, the PMMA/graphene film was merged into DI water to clean the residues. The PMMA/graphene was then rinsed in DI water for several times and attached to sapphire substrates. After drying in air through baking at 170 ºC for 5 min, the PMMA was removed by hot acetone.

Characterization. The prepared samples were characterized using SEM (Hitachi S-4800, operating at 1 kV), Raman spectroscopy (WITec alpha300 RS). The cross-TEM sample was fabricated using a focused ion beam system (FIB, FET Strata DB 235). The TEM and SAED were performed on TEI Tecnai F20 at 200 kV, and the STEM was acquired using FEI cubed double corrected Themis G2300 operated at 300 kV. AFM morphology image was carried out on a Bruker Dimension Icon. The XRD was measured with Rigaku (D/MAX 2500PC).

ASSOCIATED CONTENT

Supporting Information. The supporting data and DFT calculations are included. This material is available free of charge via the Internet at http://pubs.acs.org.

AUTHOR INFORMATION

Corresponding Authors

*zfliu@pku.edu.cn;

*tbwei@semi.ac.cn;
*p-gao@pku.edu.cn;
*jmli@semi.ac.cn;
*yujie_wei@lnm.imech.ac.cn

ACKNOWLEDGMENTS

Y. Qi, Y. Y. Wang, Z. Q. Pang, Z. P. Dou contributed equally to this work. This work was financially supported by the National Key R&D Program of China (No. 2018YFB0406703), the National Natural Science Foundation of China (Nos. 51432002, 61474109, 51290272, 51502007, 11474247, 51672007 and Y761020000), National Equipment Program of China (ZDYZ2015-1), Beijing Municipal Science and Technology Planning Project (Nos. Z161100002116020, Z161100002116032), and Beijing Natural Science Foundation (No.4182063). P. G. also thanks the support from the National Program for Thousand Young Talents of China and "2011 Program" Peking-Tsinghua-IOP Collaborative Innovation Center of Quantum Matter. We acknowledge Electron Microscopy Laboratory in Peking University for the use of Cs corrected electron microscope.

REFERENCES

1. Nakamura, S.; Mukai, T.; Senoh, M. *J.Appl. Phys.* **1994**, *76*, 8189-8191.

2. Nakamura, S.; Krames, M. R. *P. Ieee* **2013**, *101*, 2211-2220.

3. Nakamura, S.; Senoh, M.; Nagahama, S.; Iwasa, N.; Yamada, T.; Matsushita, T.; Kiyoku, H.; Sugimoto, Y. *Jpn. J. Appl. Phys.* **1996**, *35*, L74-L76.

4. Kneissl, M.; Kolbe, T.; Chua, C.; Kueller, V.; Lobo, N.; Stellmach, J.; Knauer, A.; Rodriguez, H.; Einfeldt, S.; Yang, Z.; Johnson, N. M.; Weyers, M. *Semicond. Sci. Tech.* **2011**, *26*, 014036.

5. Binari, S. C.; Redwing, J. M.; Kelner, G.; Kruppa, W. *Electron. Lett.* **1997**, *33*, 242-243.

6. Mishra, U. K.; Parikh, P.; Wu, Y. F. *P. Ieee* **2002**, *90*, 1022-1031.

7. Hemmingsson, C.; Paskov, P. P.; Pozina, G.; Heuken, M.; Schineller, B.; Monemar, B. *J. Cryst. Growth* **2007**, *300*, 32-36.

8. Zhang, J. X.; Qu, Y.; Chen, Y. Z.; Uddin, A.; Yuan, S. *J. Cryst. Growth* **2005**, *282*, 137-142.

9. Ponce, F. A.; Krusor, B. S.; Major, J. S.; Plano, W. E.; Welch, D. F. *Appl. Phys. Lett.* **1995**, *67*, 410-412.

10. Nakamura, S. *Science* **1998**, *281*, 956-961.

11. Schubert, M. F.; Chhajed, S.; Kim, J. K.; Schubert, E. F.; Koleske, D. D.; Crawford, M. H.; Lee, S. R.; Fischer, A. J.; Thaler, G.; Banas, M. A. *Appl. Phys. Lett.* **2007**, *91*, 231114.

12. Hemmingsson, C.; Pozina, G. *J. Cryst. Growth* **2013**, *366*, 61-66.

13. Rosner, S. J.; Carr, E. C.; Ludowise, M. J.; Girolami, G.; Erikson, H. I. *Appl. Phys. Lett.* **1997**, *70*, 420-422.

14. Sugahara, T.; Sato, H.; Hao, M. S.; Naoi, Y.; Kurai, S.; Tottori, S.; Yamashita, K.; Nishino, K.; Romano, L. T.; Sakai, S. *Jpn. J. Appl. Phys.* **1998**, *37*, L398-L400.

15. Liu, L.; Edgar, J. H. *Mat. Sci. Eng. R.* **2002**, *37*, 61-127.

16. Meng, W. J.; Perry, T. A. *J. Appl. Phys.* **1994**, *76*, 7824-7828.

17. Kim, C.; Robinson, I. K.; Myoung, J.; Shim, K. H.; Kim, K. *J. Appl. Phys.* **1999**, *85*, 4040-4044.

18. Mathis, S. K.; Romanov, A. E.; Chen, L. F.; Beltz, G. E.; Pompe, W.; Speck, J. S. *J. Cryst. Growth* **2001**, *231*, 371-390.

19. Haffouz, S.; Lahreche, H.; Vennegues, P.; de Mierry, P.; Beaumont, B.; Omnes, F.; Gibart, P. *Appl. Phys. Lett.* **1998**, *73*, 1278-1280.

20. Datta, R.; Kappers, M. J.; Vickers, M. E.; Barnard, J. S.; Humphreys, C. J. *Superlattice. and Micro.* **2004**, *36*, 393-401.

21. Deng, B.; Pang, Z.; Chen, S.; Li, X.; Meng, C.; Li, J.; Liu, M.; Wu, J.; Qi, Y.; Dang, W.; Yang, H.; Zhang, Y.; Zhang, J.; Kang, N.; Xu, H.; Fu, Q.; Qiu, X.; Gao, P.; Wei, Y.; Liu, Z.; Peng, H. *ACS Nano* **2017**, *11*, 12337-12345.

22. Li, B. W.; Luo, D.; Zhu, L.; Zhang, X.; Jin, S.; Huang, M.; Ding, F.; Ruoff, R. S. *Adv. Mater.* **2018**, *30*, 1706504.

23. Xu, X.; Zhang, Dong, Z.; J.; Yi, D.; Niu, J.; Wu, M.; Lin, L.; Yin, R.; Li, M.; Zhou, J.; Wang, S.; Sun, J.; Duan, X.; Gao, P.; Jiang, Y.; Wu, X.; Peng, H.; Ruoff, R. S.; Liu, Z.; Yu, D.; Wang, E.; Ding, F.; Liu, K. *Sci. Bull.* **2017**, *62*, 1074-1080.

24. Leszczynski, M.; Teisseyre, H.; Suski, T.; Grzegory, I.; Bockowski, M.; Jun, J.; Porowski, S.; Pakula, K.; Baranowski, J. M.; Foxon, C. T.; Cheng, T. S. *Appl. Phys. Lett.* **1996**, *69*, 73-75.

25. Tanaka, M.; Nakahata, S.; Sogabe, K.; Nakata, H.; Tobioka, M. *Jpn. J. Appl. Phys.* **1997**, *36*, L1062-L1064.

26. Alaskar, Y.; Arafin, S.; Wickramaratne, D.; Zurbuchen, M. A.; He, L.; McKay, J.; Lin, Q.; Goorsky, M. S.; Lake, R. K.; Wang, K. L. *Adv. Funct. Mater.* **2014**, *24*, 6629-6638.

27. Chan, K. T.; Neaton, J. B.; Cohen, M. L. *Phys. Rev. B* **2008**, *77*, 235430.

28. Al Balushi, Z. Y.; Miyagi, T.; Lin, Y.-C.; Wang, K.; Calderin, L.; Bhimanapati, G.; Redwing, J. M.; Robinson, J. A. *Surf. Sci.* **2015**, *634*, 81-88.

29. Kim, J.; Bayram, C.; Park, H.; Cheng, C.-W.; Dimitrakopoulos, C.; Ott, J. A.; Reuter, K. B.; Bedell, S. W.; Sadana, D. K. *Nat. Commun.* **2014**, *5*, 4836.

30. Chung, K.; Lee, C.-H.; Yi, G.-C. *Science* **2010**, *330*, 655-657.

31. Li, X. S.; Cai, W. W.; An, J.; Kim, S.; Nah, J.; Yang, D. X.; Piner, R.; Velamakanni, A.; Jung, I.; Tutuc, E.; Banerjee, S. K.; Colombo, L.; Ruoff, R. S. *Science* **2009**, *324*, 1312-1314.

32. Wu, X. H.; Fini, P.; Tarsa, E. J.; Heying, B.; Keller, S.; Mishra, U. K.; DenBaars, S. P.; Speck, J. S. *J. Cryst. Growth* **1998**, *189*, 231-243.

33. Lang, T.; Odnoblyudov, M. A.; Bougrov, V. E.; Romanov, A. E.; Suihkonen, S.; Sopanen, M.; Lipsanen, H. *Phys. Status Solidi A.* **2006,** 203, R76-R78.

34. Sugawara, Y.; Ishikawa, Y.; Watanabe, A.; Miyoshi, M.; Egawa, T. *Jpn. J. Appl. Phys.* **2016**, *55*, *05FB08*.

35. Lee, J. E.; Ahn, G.; Shim, J.; Lee, Y. S.; Ryu, S.; *Nat. Commun.* **2012**, *3*, 1024.

36. Trodahl, H. J.; Martin, F.; Muralt, P.; Setter, N. *Appl. Phys. Lett.* **2006**, *89*, 3498.

37. Prokofyeva, T.; Seon, M.; Vanbuskirk, J.; Holtz, M.; Nikishin, S. A.; Faleev, N. N.; Temkin, H.; Zollner, S. *Phys. Rev. B* **2001**, *63*, 157.

38. Sarua, A.; Kuball, M.; Van Nostrand, J. E. *Appl. Phys. Lett.* **2002**, *81*, 1426-1428.

39. Kadleikova, M.; Breza, J.; Vesely, M. *Microelectron. J.* **2001**, *32*, 955-958.

40. Davydov, V. Y.; Kitaev, Y. E.; Goncharuk, I. N.; Smirnov, A. N.; Graul, J.; Semchinova, O.; Uffmann, D.; Smirnov, M. B.; Mirgorodsky, A. P.; Evarestov, R. A. *Phys. Rev. B* **1998**, *58*, 12899-12907.

41. Ni, Z. H.; Yu, T.; Lu, Y. H.; Wang, Y. Y.; Feng, Y. P.; Shen, Z. X. *ACS Nano* **2008**, *2*, 2301-2305.

42. Zabel, J.; Nair, R. R.; Ott, A.; Georgiou, T.; Geim, A. K.; Novoselov, K. S.; Casiraghi, C. *Nano Lett.* **2012**, *12*, 617-621.

Table of content